www.revistageintec.net
ISSN: 2237-0722
revista GEINTEC Gestão, Inovação e Tecnologias

Coating of Inconel 718 Super Alloy with Stellite6 Cobalt-base Alloy Coated Layer via Tig Welding Process & Investigating the its Erosion Resistance & Hardness Behavior

Behnam Gandomkar[1]

[1]Mechanical Engineering, Najafabad Branch, Islamic Azad University, Najafabad, Isfahan, Iran.

[1]gandomkar@aftermail.ir

Abstract

Heat treatable nickel-based super alloys have appropriate wear resistance to sweet and sour wear environments. Therefore, they are used in disparate industries such as petroleum, gas, and transportation. These super alloys have appropriate hardness, however, sometimes in the oil, gas, and military of this super alloy, more hardness is required to increase erosion resistance. Hence, it is efficient to apply cladding on the super alloy by cobalt-based super alloys.

Surface cladding is one of the appropriate methods for increasing the service life of this class of cobalt-based super alloys is used. In the present research, Incoloy 718 were coated with stellite6 cobalt-based super alloys through GTAW method and examined the effect of TIG welding process parameters were examined on hardness and erosion resistance by conducting investigations such as Metallography, microhardness testing, SEM microscope analysis and erosion experiments.

The results demonstrated that hardness and erosion resistance of the weld metal from surface to the depth of weld toes increased gradually. The gradual decrease of hardness of weld metal is pertinent to the reduction of the size and quantity of NbC and cobalt. Besides, by increasing the welding current (heat input) preheating temperature, the hardness and resistance to erosion in weld metal was decreased and increased, respectively. Upon increasing the intensity of the welding current and the number of coating layers the dilution value of the base metal in weld metal increases and decreased, receptively. By increasing of preheat temperature, the input value of the basic metal element decreased in coating layer.

Finally, the highest erosion resistance is pertinent to the coated samples in 1. triple layer coating, 2. coated sample in the lowest welding current, 3. coated sample in the at 200 and 300 degrees centigrade preheating temperature.

Key-words: TIG Welding, GTAW Method, Stellite6 Cobalt, Inconel 718.

1. Introduction

Nickel-based super alloys have effective strength in higher melting point 1 in comparison to other super alloys, therefore, weldability of alloys, especially super alloys with respect to their chemical compound, crystal structure, morphology, stability, plus the effect of disparate factors on them as a background for studying the properties of welding is inevitable [1]. A super alloy is developed to be used in high temperature, normally it is based on elements of group VII, where the intense mechanical stress occur and surface smoothness and uniformity is required [2]. Nickel-based alloys usually maintain their strength up to 650 degrees centigrade. However, in the higher temperatures they lose their strength rapidly [3]. High-performance super alloys possess perfect mechanical strength and creep resistance in higher temperature, higher fatigue life, fuzzy stability, surface stability, and erosion resistance, and good oxidation [4]. Ni-Cr alloys were the first nickel-based hard-coated alloy in different industries, which were replaced with cobalt-based alloys. This super alloy can be used in wider range of the corrosive environment due to its higher wear resistance [5]. Nickel-based alloys are designated under trade name on the basis of the application of the alloy matters in their structure. Two important classes of them that are mentioned herein below are Monel and Inconel [6]. Inconel is a trade name designated on the nickel-based Austenite alloys containing chrome [7]. Inconel 718 is a nickel-based super alloy with high strength and appropriate wear resistant in the sour and sweet corrosive environment. Therefore, nowadays it has a broad application in the oil and marine industries [8]. The cracks resulting from the heat treatments after welding (PWHT) that occur to the nickel-based precipitation hardening super alloys, are called strain age cracking (SAC) as well. The characteristics of this phenomenon are different in various super alloys [9]. In order to have the desired fatigue and heat properties in higher temperature, in the radial forging dies, at first, shielded metal arc welding (SMAW) with the nickel base electrode, a flexible and mediatory layer was deposited on the surface of the aforesaid dies, and the second layer was deposited on the surface of the welded layer through gas tungsten arc welding (GTAW) and using Udimet 520 nickel based welding wire [10]. IN718 alloy that hardens with Niobium deposit, which has a high weldability. Since its sedimentation is carried out slowly, the hardening sediment alloys with aluminum and titanium, cover a faster sedimentation reaction when placed in the average thermal range, this rapid reaction results in the sever crack problem in welding or repair welding of these super alloys [11]. In welding super alloys using methods with high density is emphasized. In most applications, TIG method is preferred due to its capability in welding the thin points is preferred. The argon shielding gas or its combination with helium is normally used. Repairing the

super alloy parts contain fewer alloys were used traditionally through GTAW process [12]. Most of the casting super alloys with the coaxial grains are repaired using GTAW welding. However, soldering, penetration connections, laser welding, and electron radiation are used as well [13]. Ni-Cr-Mo alloys were the first alloys of solid solution used in disparate industries. These alloys are used in the application that needs high resistance to wear [14]. Inconel alloy 625 from this group is resistant to typical wear and pitting. Inconel 625 is highly resistant to heat, perfect resistant to wear, and good welding [15 and 16]. The microscopic structure of Inconel alloy 625 after coating on a martensitic stainless steel is dendritic and some of the carbide sediments appear in them. These sediments are rich in niobium and the value of these mixes is few [17]. Stellites are the first cobalt-based alloys used in the hardening. At first, Co-Cr-W-C alloys were used for coating the surface of the variety of steels in different industries for resistance to heat, wear, and oxidation [18]. Due to their broad freezing range, Stellites possess hot cracking more than Inconel alloy 625 [19]. The crack is formed on account of the remaining tensile stress in the region affected by heat, the coated samples with cobalt-based super alloys [20]. The process of coating with oxygen is one of the more advanced methods is the process of heat spray. Adding chrome to cobalt-tungsten carbide powder is preferred when the wear resistance is more crucial [21-23]. Welding with neuter shielding gas is one of the usual methods used for improving the surface properties of various types of HTLA steels [24]. GMAW method is one of the welding methods used for improving the surface properties of various types of HTLA steels [25]. The modified type of this method is called U GMAW which is known as Universal GMAW. The welding torch used in this process increased the capability of GMAW process by controlling the welding variables [24]. From the metallurgic viewpoint, using the pulse current on surface in the welding processes results in creation of fine-grained structure, which is due to the turbulence of the melted pool [26 and 27]. During coating of the heat treatment low alloy steels (HTLA) with the welding methods few factors must be taken into account [28]. High welding speed can lead to increase of dilution and has destructive effects on coating. The higher speed of welding causes more melting of the base, consequently, by the increase of the penetration of the elements from the base into the cover, the dilution increases [29]. Besides, using pulse current in the plasma arc welding method results in smaller structure, higher hardness, and less dilution. Using the fluctuating current leads to creation of broad weld toe and reduction of the depth of penetration, thus, the dilution decreases [30].

2. Methods & Materials

2.1. Raw Materials

In the present article, Incology 718 super alloy as sublayer and the welding rod made of Stellite 6 cobalt-based super alloy were used. This cobalt and nickel-based super alloy was used mostly in the natural oil and gas industry facilities in the marine shafts.

The chemical compound and other characteristics of consumed products such as diameter and AWS standard properties of welding rods is displayed in Table 1.

Table 1 - Chemical Compound of Consumed Matters

Alloy	AWS	قطر(mm)	Ni	Cr	Fe	Mo	Ti	Al	C	Co
Incoloy 718	--	--	52/7	18/3	18/9	3	1	0/49	0/02	0/20
Stellite 6	ERCocr-A	3mm	2/14	30/10	2/19	0/31	--	--	1/28	--

2.2. Sample Layering

To investigate the effect of the respective variables (input heat, preheating temperature, and coating thickness) on the microstructure, hardness, and strength to erosion by the GTAW process, seven Iconology 718 samples with heat treatment were provided in the dimensions of 10*10*10 mm. the prepared samples were heat treated using the following method.

Solution Treatment: solution at the temperature of 1021-1052 degrees centigrade for 1-2 hours cooling by air.

Participation hardness treatment: at the temperature of 774-802 degrees centigrade for 6-8 hours to be cooled by air.

Table 2 - Particulars of the Provided Samples

Sample No.	No. of Layers	Layer Thickness (mm)	Current (A)	Preheating Temperature
1	1	2.4	220	200
2	1	2.4	250	200
3	1	2.4	290	200
4	2	4.3	250	200
5	3	6.2	250	200
6	1	2.4	250	--
7	1	2.4	250	300

After completion of layering and when the coated samples were cooled up to the environment temperature, the layered samples were examined by ultrasonic testing and penetration liquid to ensure formation of coating without crack. When welding some waste stress remained in the samples, which can lead to problems such as crack, etc. at the subsequent stages. Consequently, to free these waste stresses, the respective samples underwent stress relieving treatment for 30 minutes at the 600 degrees centigrade.

2.3. Preparing Samples

Incoloy 718 sample without coating and the layered samples underwent preparation treatment to determine the chemical analysis, metallography, test hardness, and erosion tests.

2.4. Metallography & Hardness Testing

At first, the level and point of the prepared samples were polished with sandpapers containing SiC particles up to mesh of 1200. Then, they were varnished by alumina powder with mesh of 0.03 μm. After preparation, the microstructure of the samples were examined using optical and electron microscopes. To determine the chemical compound of metal weld phase, EDS analysis PMI device (Razi Research Center) were used. Besides, the hardness testing of the samples were carried out by a microhardness tester containing indenter Vickers, then, it was illustrated.

2.5. Erosion Test

Erosion behavior of the samples was investigated using the pin-on-disk wear test and in accordance with ASTM G99 standard. In this method, the respective sample underwent pin-on-disk erosion test made of hardened steel containing 55 HRC. All tests were conducted by erosion test device at Razi Metallurgical Research Center.

3. Results

3.1. Sample Layering Results

The results of layering the samples including coating layers, the value of elements affecting on the mechanical properties of the samples are presented in Table 3. The table shows that the

percentage of base metal elements decreases by the increase of the number of the coated layers, increases by the increase of the intensity of the welding current, and decreases by the increase of the preheating temperature. The results demonstrated that in Table 3 are displayed in the Diagrams of Figure 3.

Table 3 - The Value of Factors affecting the Mechanical Properties of Samples

#	Alloy Coating	No. of Layers	Analysis			
			Ni	Co	Cr	Fe
1		(220A)1	25.89	23.01	23.62	11.37
2		(250A)1	34.35	20.90	23.90	12.53
3		(290A)1	35.01	22.23	29.74	12.70
4	Stellite6	(200 preheating degree)2	11.70	45.33	27.41	5.81
5		(200 preheating degree)3	7.63	49.44	23.97	4.12
6		(without preheating)1	26.40	32.62	25.96	12.58
7		(300 preheating degree)1	25.01	29.98	23.01	10.20

3.2. Microstructure of Samples by Optical Microscope

In this chapter, the microstructure of the welded samples was studied in various conditions by optical microscope.

3.2.1. Coating Microstructure in the Intensity of Various Welding Currents

Figure 1 - Optical Microscopic Image of Stellite 6 Alloy Surface on Inconel 718 in Disparate Currents a. 200 Amp, b. 250 Amp, c. 290 Amp (*200)

Received: 26.04.2021 – Accepted: 15.05.2021

Figure 3.2. is an optical microscopic image of the etched level of satellite coating on Inconel 718 in the single-layer coating in three different current intensity. Figure 1 (a) is an optical microscopic image of the current intensity of 200 Amp and Figure 1 (b) and (c) are optical microscopic images in the current intensity of 250 and 290 Amp. As shown herein below, all samples show dendrite microstructure.

Figures show that by increasing the current the dendrite size increases, this increase from sample a to sample b was visible, however, it was little from b to c sample and it is not quite visible. This increase of the size of the dendrites increases by the increase of the intensity of the welding current (input heat).

3.3. Microstructure of Coating Samples in Disparate Layers

Figure 2 is an optical microscopic image of the etched surface, Stellite 6 coating on Inconel 718 in disparate number of layers. Figure 2a, is an optical microscopic image of the first layer of Stellite 6 alloy and Figure 2b and c are optical microscopic images of the second and thirds layers. The Figure shows that all samples have dendrite structure.

Figure 2 - Optical Microscopic Image of Stellite 6 in Disparate Layers a. Single-Layer Coating, b. Double-Layer Coating, c. Triple-Layer Coating (*400)

3.4. Microstructure of Coating Samples in Disparate Preheating

Figure 3. is an optical microscopic image of the etched surface of Stellite 6 coating on Inconel 718 in different preheating temperature. Figure 3a is an optical microscopic image in the preheating temperature of 200 degrees centigrade and Figure 2b and c are optical microscopic images of samples without preheating and 300 degrees centigrade. The Figures show that all samples have dendrite structure.

Figure 3 - Optical Microscopic Image of Stellite 6 Coating Surface in Disparate Preheating Temperatures a. 200, b. without Preheating, c. 300 Degrees Centigrade

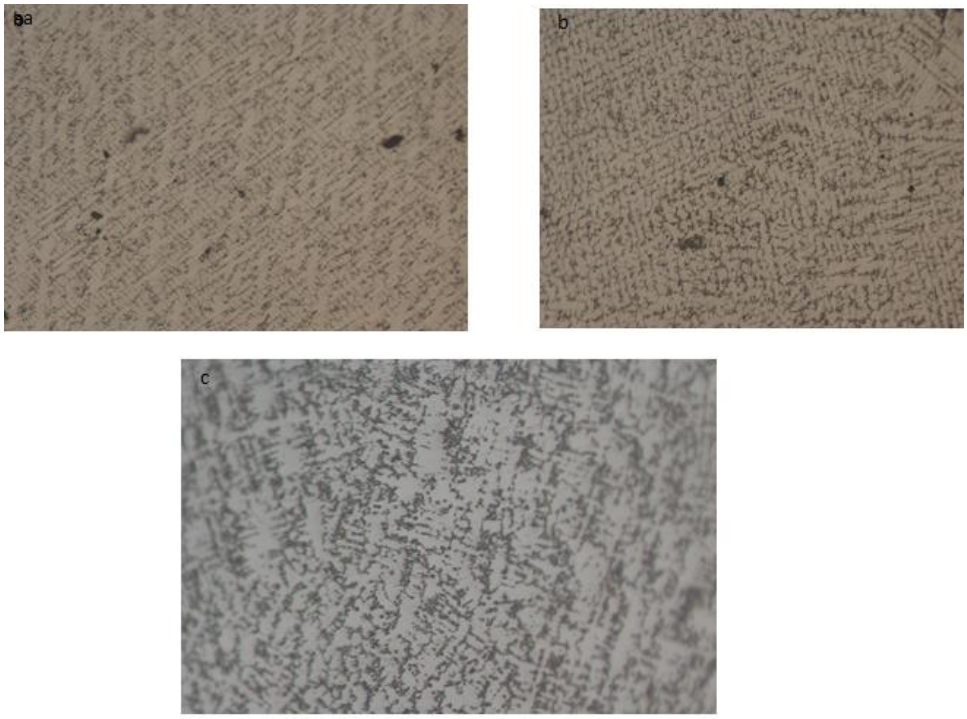

3.5. Results of Microscopic Images of SEM and EDS Analysis of Samples with Disparate Current Intensity

Analysis and EDS graphs of disparate regions are specified and designated, Stellite 6 coating plus back-scattered electron image and analyzed points are shown in Figures 4 to 6. Investigating the results of analysis of D points from the samples of 200 and 250 Amp and the analysis of C point from the sample 290 Amp with base phase indicated that by increasing the current intensity, the value of nickel, chrome, and iron increased as well. All light points in the samples are rich in niobium and their values were different in various points.

Figure 4 - Analysis & SEM Image of Samples with Current Intensity of 200 Amp

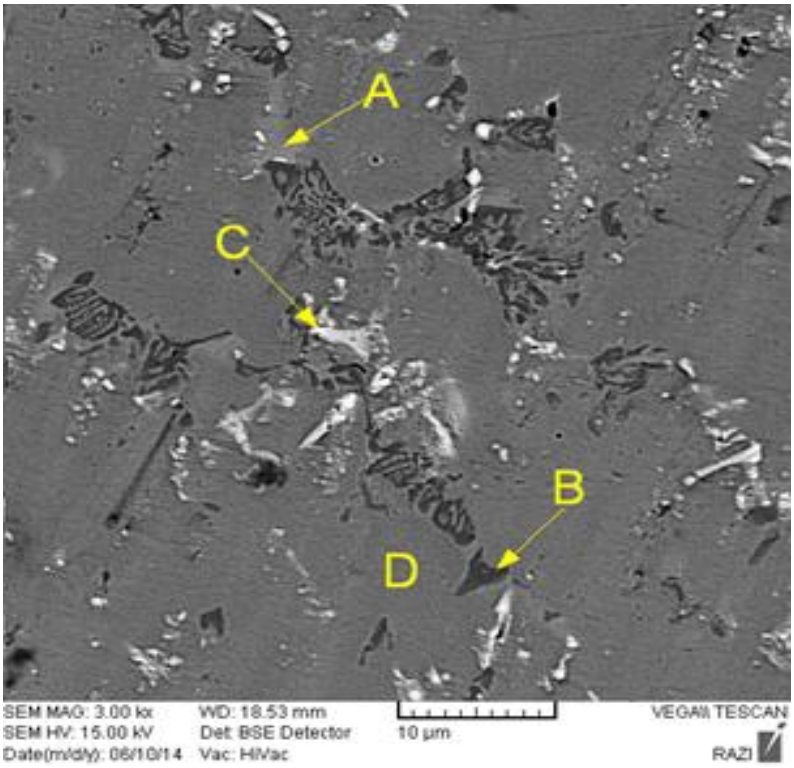

Figure 5 - Analysis & SEM Image of Sample in Current Intensity of 250 Amp

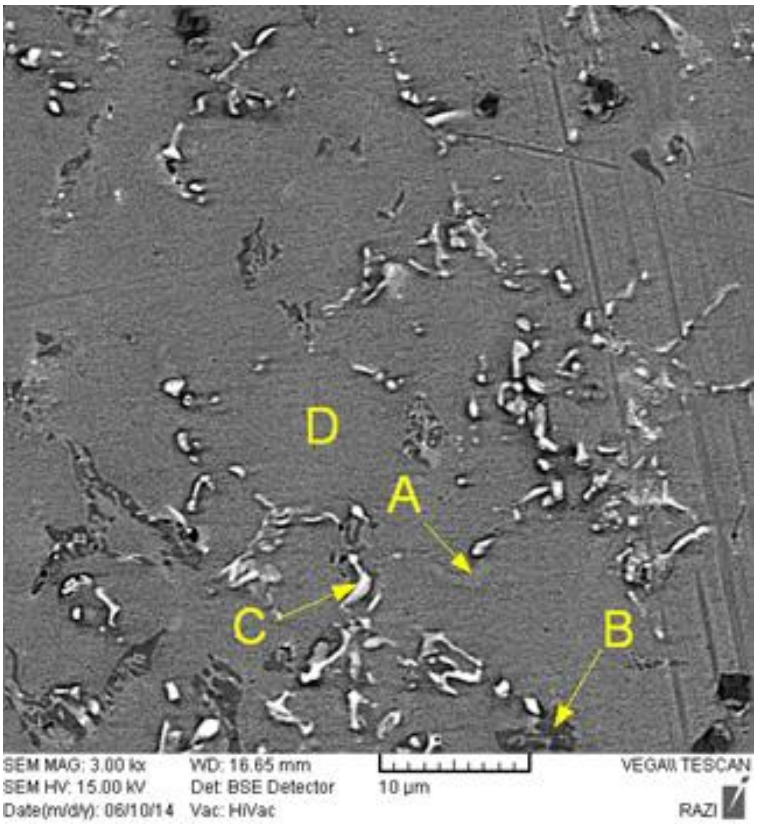

Received: 26.04.2021 – Accepted: 15.05.2021

Figure 6 - Analysis and SEM Image of Sample with Current Intensity of 290 Amp

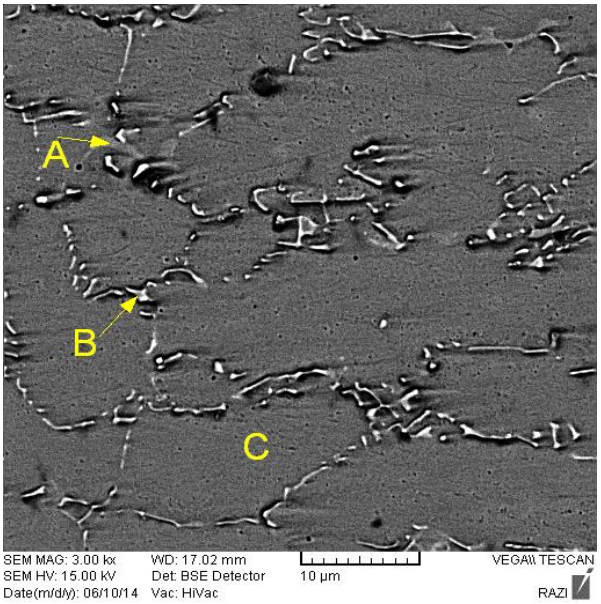

3.6. Results of SEM Microscopic Images and EDS Analysis of Stellite 6 Coating in Different Number of Layers

The EDS analysis of the various Stellite 6 coating regions in different layers plus the back-scattered electron images and the analysis points are displayed in Figures 7 to 9. According to Figures, by increasing the number of layers, the percentage of nickel and chrome are decreased and the percentage of cobalt increases.

Figure 7 - Image of Back-Scattered Electrons & EDS Analysis of the Single-Layer Coat

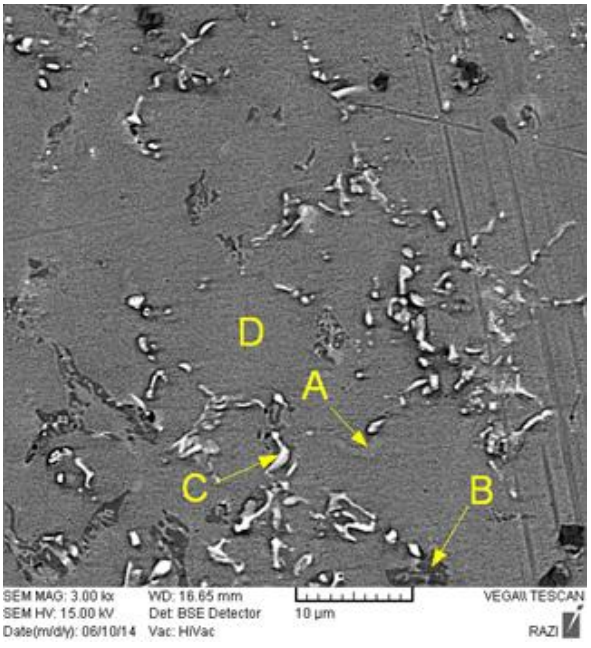

Received: 26.04.2021 – Accepted: 15.05.2021

Figure 8 - Image of Back-Scattered Electrons & EDS Analysis of the Double-Layer Coat

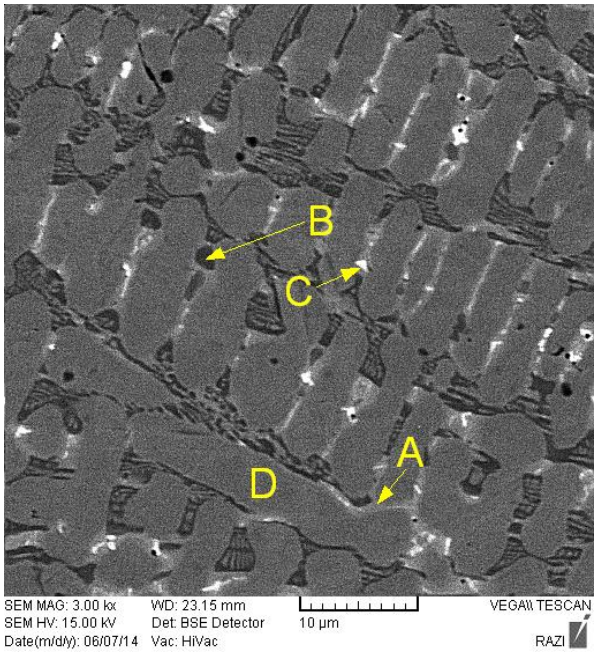

Figure 9 - Image of Back-Scattered Electrons & EDS Analysis of the Triple-Layer Coat

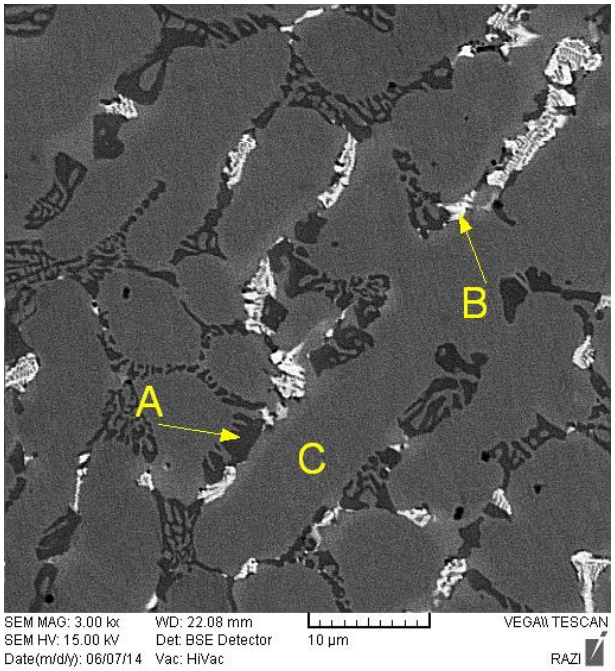

3.7. The Results of SEM Images and EDS Analysis of Samples with Disparate Preheating Temperature

EDS analysis of various Stellite 6 coating analysis in different preheating temperatures plus back-scattered electrons and analysis of the points are displayed in Figures 10, 11, and 12.

Figure 10 - Analysis & SEM Image of Samples with Preheating Temperature of 200 Degrees Centigrade

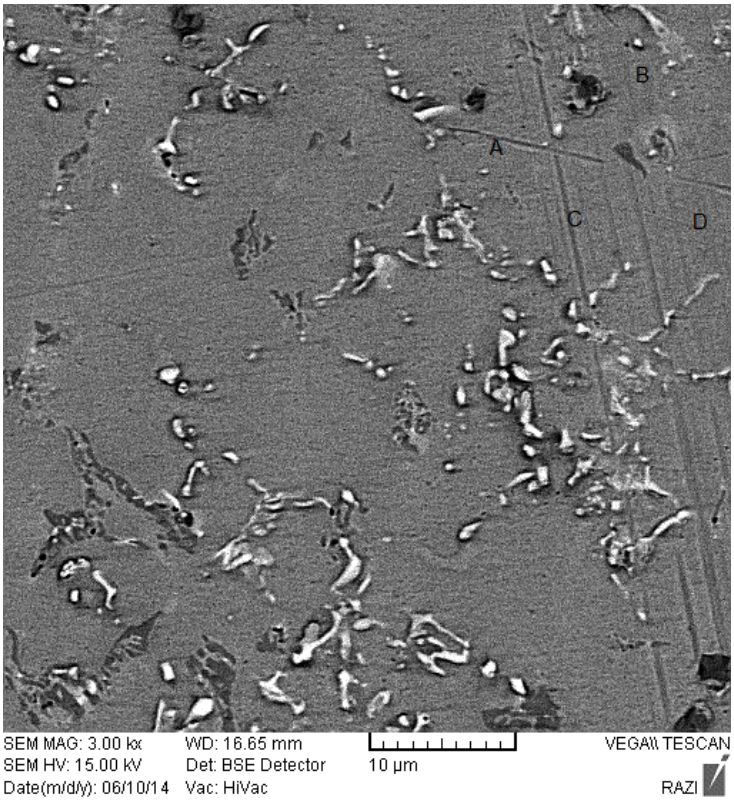

Figure 11 - Analysis & SEM Image of Samples with Preheating Temperature of 300 Degrees Centigrade

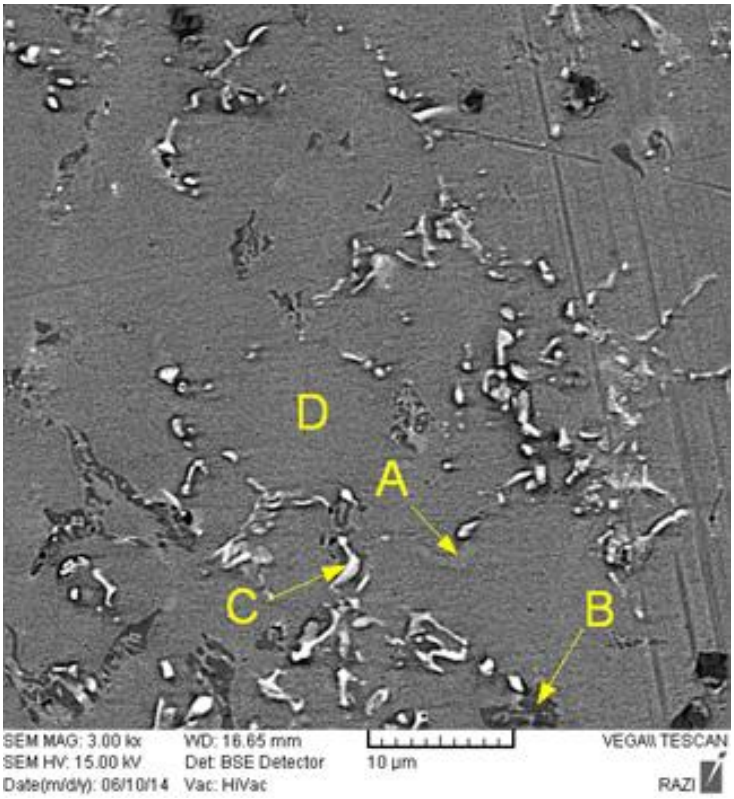

Figure 12 - Analysis & SEM Image of Samples without Preheating Temperature

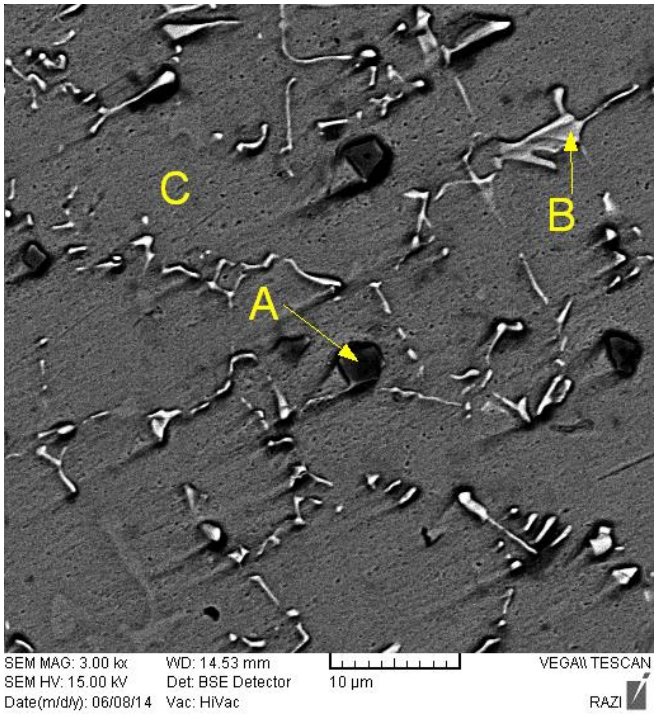

3.8. Microhardness Test Results

The results of microhardness test from depth to surface in weld metal, the area of combination of the weld metal and base metal as hardness profile for coated samples in different current intensities in Figure 13, the different layer numbers in Figure 14, and different preheating temperatures are displayed in Figure 15.

Figure 13 - Profile of Microhardness of Stellite 6 Coating of Intensity of Various Welding Currents

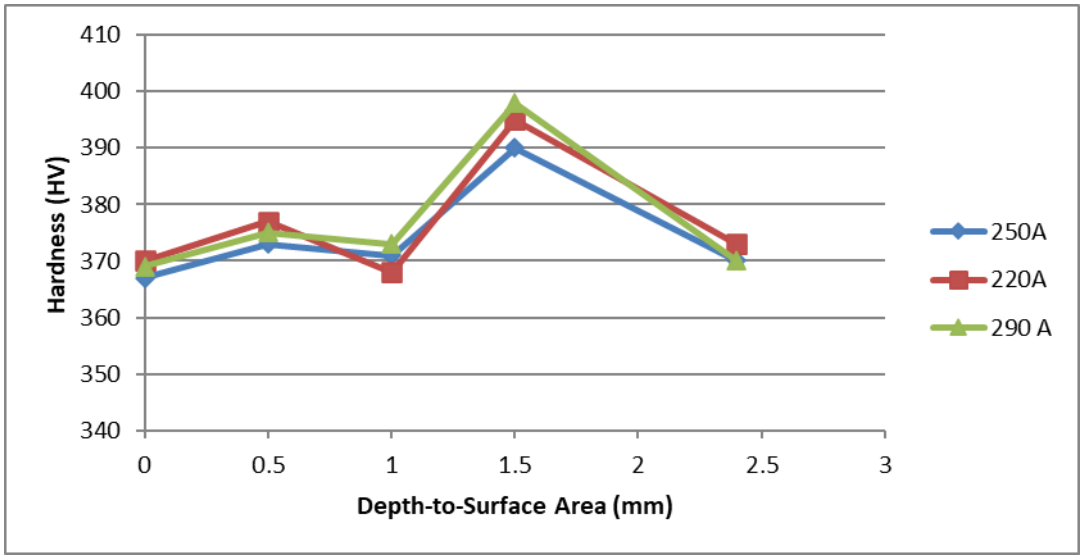

Received: 26.04.2021 – Accepted: 15.05.2021

Figure 14 - Profile of Microhardness of Stellite 6 Coating of Intensity of Various Coating Layers

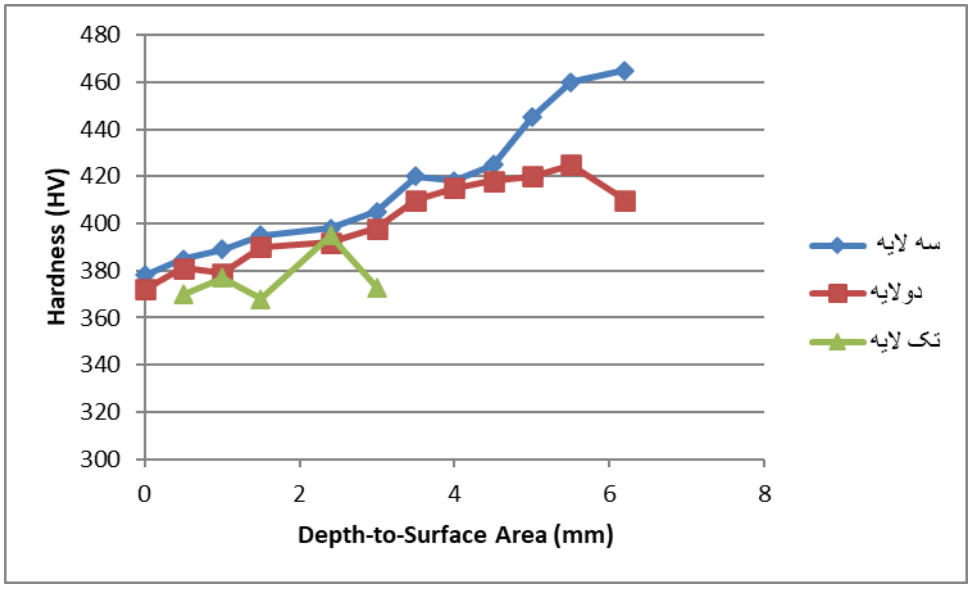

Figure 15 - Profile of Microhardness of Stellite 6 Coating in Various Preheating Temperatures

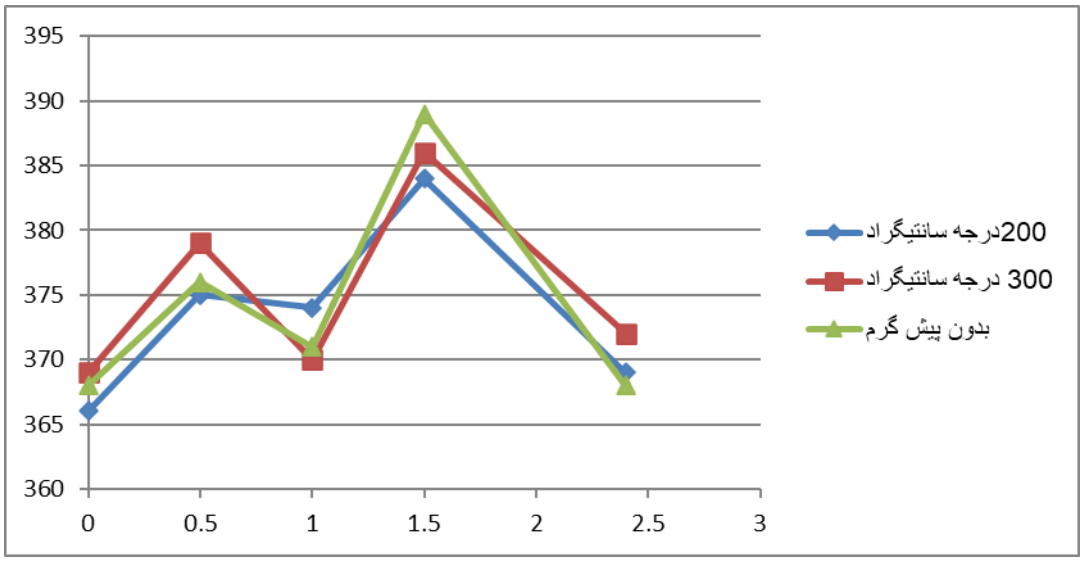

3.9. Erosion Test

The results of erosion test of the different samples are displayed in Tables 4 to 12, which include the results of erosion test in accordance with ASTM standard that contains the following conditions.

Test Reference Standard: ASTM G99-05

- Abrasive Surface: Steel disk with hardness of 55HRC
- Imposed Stress: 10 KPa
- Linear Velocity: 10 m/min

The results of test are as follows:

Table 4 - The Results of Erosion Test According to ASTM Standard for Base Metal Sample

Travelled Distance (m)	600	1200	1800	2400	3000
Weight Loss (mg)	22.5	55.8	88.3	125.8	135.2

Table 5 - Results of Erosion Test in Accordance with ASTM G99 Standard for Samples with Current Intensity of 200 Amp

Travelled Distance (m)	600	1200	1800	2400	3000
Weight Loss (mg)	7.5	31.7	41.6	71.4	79.18

Table 6 - Results of erosion Test in accordance with ASTM G99 Standard for Samples with Current Intensity of 250 Amp

Travelled Distance (m)	600	1200	1800	2400	3000
Weight Loss (mg)	7.8	33.2	42.5	72.1	81.3

Table 7 - Results of Erosion Test in Accordance with ASTM G99 Standard for Samples with Current Intensity of 290 Amp

Travelled Distance (m)	600	1200	1800	2400	3000
Weight Loss (mg)	7.9	33.3	43.8	72.9	82.1

Table 8 - Results of Erosion Test in Accordance with ASTM G99 Standard for Samples without Preheating Temperature

Travelled Distance (m)	600	1200	1800	2400	3000
Weight Loss (mg)	7.8	33.1	43.5	73.01	82.3

Table 9 - Results of Erosion Test in Accordance with ASTM G99 Standard for Samples with Preheating Temperature of 200 Degrees Centigrade

Travelled Distance (m)	600	1200	1800	2400	3000
Weight Loss (mg)	7.8	33.2	42.5	72.1	81.3

Table 10 - Results of Erosion Test in Accordance with ASTM G99 Standard for Samples with Preheating Temperature of 300 Degrees Centigrade

Travelled Distance (m)	600	1200	1800	2400	3000
Weight Loss (mg)	7.9	33.1	42.7	71.9	81.7

Table 11 - Results of Erosion Test in Accordance with ASTM G99 Standard for Double-Layer Coating Samples

Travelled Distance (m)	600	1200	1800	2400	3000
Weight Loss (mg)	5.1	17.5	38.1	51.5	67.2

Table 12 - Results of erosion Test in accordance with ASTM G99 Standard for Triple-Layer Coating Samples

Travelled Distance (m)	600	1200	1800	2400	3000
Weight Loss (mg)	3.1	12.4	26.3	39.6	53.7

4. Result & Discussion

4.1. Examining the Results of Analysis of Weld Samples

By analyzing three samples with different amperes, it can be concluded that by increasing the ampere, the input heat to weld region and more quantities of alloy elements of base metal enter the coating. The results indicated that in higher amperes the quantities of elements such as Ni, Fe, and Cr increase. Therefore, increase of the ampere is directly related to the increase of the percentage of the base metal in the coating.

In different preheating temperatures, the results indicated that by increasing the preheating temperature the possibility of the elements of the base metal's entering the coating in low and the input heat has less effective. For instance, in the preheating temperature of 200 and 300 degrees centigrade, fewer base elements enter the coating. The results of the double-layer and triple-layer samples revealed that by increasing the number of coating layers, the quantity of the elements of the base metal was decreased considerably and the coating alloy elements were increased.

4.2. Examining the Results of Optical Microscope (Dendrite Structure in Weld Metal)

The microstructures of welded Stellite 6 on Inconel 718 in the unbalanced cooling condition is similar to welding, including dendrites plus a distribution of carbides. High freezing velocity and more heat slope in the melted material is among the major differences of freezing in welding and casting, which demonstrates that a great part of the coating structure is dendrite and created in cellular forms in the area of interface [31].

In welding nickel-based super alloys most of the coaxial grains are not visible. The major reason is that for the formation of the coaxial region the dendrite pieces that are created due to remelting or the fracture must remain in the melted matter without melting away from the interface, in which the high temperature of the center of the melting pool makes it difficult [32].

The dendrite formed in sample No. 1 is relatively small. The coating layer is created in the sample No. 1 with the minimum input heat (Table 3-2). The less input heat leads to reduction of the dimensions of the melting region, consequently, the volume of the melt pool decreases. The small volume of the melt pool in comparison to the base metal volume, which has the role of heat sink for the weld metal, can lead to increase of the freezing rate in the weld metal. This increase of freezing rate results in shrinking the dendrites [33].

In accordance with the primary foundations of freezing, the morphology of the frozen matter is controlled by the heat gradient (G) in the melt pool close to the interface of the solidification front and growth rate (R) [59]. By reducing the G/R ratio, the microstructure of the interface is transformed from the plane state to cellular, and then, into dendrite state. In the surface, due to the contact of the melting matter with the surrounding environment (air), the freezing velocity is high and the structure turns into a very small dendrite [34].

In conducting a close comparison of the optical microscopic images pertinent to amperages of 220, 250, and 290, it was revealed that the dendrites in the weld metal of sample of 290 ampere are larger than in the sample of 220 ampere. It is due to the fact that the value of the input heat for creation of coating layer in sample of 290 ampere is more than the sample of 220 ampere, which results in increasing the dimensions of the melting region, consequently, the solidification rate of the weld metal decreases.

In the recomparison between the images of the optical microscope in the different preheating temperatures the largeness of the dendrites of the samples with the preheating temperature of 300 degrees centigrade is clearly visible, which is due to the temperature of the heat well. Consequently, the solidification rate in the weld metal decreases that it can lead to the increase in the size of the dendrites. This largeness of the structure is seen in the samples with the double-layer and triple-layer coating, which is on account of the increase in the temperature of the base metal and weld region (as the heat sink) and decrease in the solidification rate.

Heat transfer from the melt pool is carried out in two forms, i.e. through conduction and radiation. Heat transfer through conductivity is carried out by the sublayer (Inconel 718) that has relatively high heat conductivity and heat transfer through radiation is carried out by air.

4.3. Investigating the Results of the Images of SEM Microscope & EDS Analysis

The results of SEM images and EDS analysis of the samples in the amperes and coatings with different layers show the dendrite structures in the samples. On the basis of EDS analysis, the light regions are rich with niobium element and in the base regions and dendrites, the EDS analysis manifests the quantities of the base metal elements that by the increase of the ampere and input heat their quantity is increased. In general, solidification of the coating layer starts with formation of dendrite. In case the coating alloy does not contain niobium, the strengthening transformations do not occur [35]. Considering that the alloy coating contains niobium, besides, transformation, there will be other developments as well. By advancement of the solidification of the dendrites their core will be

free of carbon and niobium elements the cause of separation of these elements during solidification is related to the distribution coefficient. In case the alloy elements with distribution coefficient (K) less than the unit, thus, the poor dendrite core will be filled with these elements and the regions between the dendrites [36]. Since carbon and niobium contain distribution coefficient less that the unit. Therefore, it will not be present in the core of the dendrite. By development of the solidification with distances farther than dendrite core, carbon and niobium will continue making fractions in the liquid phase [36].

Taking into account that abrasive behavior of the coated samples is designed on the basis of the structure of the coating alloy in the welding condition. Thus, its high dilution results in the reduction of the precision in designing and reduces the lifespan of the coating layer. In general, by maintaining a low dilution value the designing can be carried out precisely. In the coating processes by welding, the number of the coating layers should be increased to resolve this deficit in order to prevent the erosion effect of dilution.

4.4. Results of Microhardness Tests

Figures 12, 13, and 14 show the distribution of hardness in the points of the coated layers. All samples show that the hardness decreased close to the surface and by distancing from the surface the hardness increased, then, decreased. Hardness drop on the surface is pertinent to reduction of niobium due to the decrease of dilution by distancing from the interface of the sublayer/overlayer and the increase of the cooling rate.

In Figure 12, the maximum hardness amounts to approximately 390-400 Vickers and by distancing from the surface the value of hardness decreases gradually up to the amount of 365-370 Vickers. Close to the interface, the value of the hardness reaches its minimum amount, which is related to dilution (reduction of the cobalt element by the increase of the ampere) and the decrease of the carbides of niobium [37]. The maximum hardness is pertinent to amperage of 220, which is due to the reduction of the quantity of nickel, iron, and chrome and the increase of cobalt element.

In Figure 13, the maximum hardness in the third layer, the value of which is 465 Vickers and it is 385 Vickers in the single layer that is on account of dilution (the increase of cobalt element in the triple-layer sample). Close to the interface, the value of hardness reaches its minimum and the maximum hardness is obtained on the weld toe.

In Figure 14, the maximum hardness is at the preheating temperature of 200 and 300 degrees centigrade that indicates that two factors of carbides of niobium and cobalt element at the preheating

temperature of 200 and 300 degrees centigrade are in the approximately similar range. It shows that at 300 and 200 degrees centigrade, the penetration of the base elements on the layer decreases. Welding without preheating the Stellite alloy is a mistake due to its fragile nature.

4.5. Investigating the Results of Erosion Test on the Samples

The results of erosion test were carried out on the samples on the basis of ASTM G99-05 standard. The results revealed that layering Stellite 6 on Inconel 718 increases the resistance to erosion, which can on account of the presence of the cobalt element in the coating. Since cobalt element is very resistant to erosion. Erosion resistance on the samples is almost the same on the different current intensities and preheating. If this resistance is increased merely in the double-layer and triple-layer samples, which is due to the considerable increase of the cobalt element in them, therefore, the triple-layer sample has the best erosion resistance among other samples.

In the samples coated with two and three Stellite layers, the percentage of the elements of coating metal is higher and the coating alloy is directed towards Stellite. Cobalt based alloys are strengthen by the carbide sediments filled with chrome and cobalt $M_{23}C_3$ and M_7C_3. The values of tungsten and molybdenum can affect their strength as well, which leads to the increase of hardness and strength, consequently, erosion resistance [38]. The most important phase created in solidification of Stellites during welding are the dendrites of gamma phase are filled with cobalt element that contain fcc structure (that is a strength structure) [39].

Therefore, in the samples with a considerable increase in the amount of cobalt, the possibility creation of gamma phase increases and leads to better conditions for erosion resistance.

One of the factors leading to creation and reduction of resistance to erosion is the role of the erosion product. The primary products of wear can be an abrasive factor and decrease the resistance to erosion of the respective piece. Therefore, one of the factors increasing the resistance to erosion in the double-layer and triple-layer samples can be pertinent to the quantity of the erosion products in the initial distances.

5. Conclusion

1. The increase of the amperage of can lead to the increase of the input heat to the workpiece and consequently, the quantity of the base elements increases in the coating.
2. The structure of coating is dendrite with regard to Figures.

3. Hardness from the interface to the weld layer surface increases, there is a little reduction merely on the surface, which can be due to the reduction of the niobium compounds.
4. In the preheating temperature 200 and 300 degrees centigrade, the maximum hardness is demonstrated, even though at the preheating temperature of 300 degrees centigrade the hardness in increased to some extent on account of entrance of the base elements.
5. Erosion resistance has a direct relationship with the value of cobalt element, therefore, the maximum erosion resistance is seen in the triple-layer samples.
6. Samples with different preheating temperatures and amperages have approximately similar erosion resistance.
7. Erosion resistance has a direct relationship with the number of the layers.

References

Sime, C.T., Hagel, W.C, *"The superalloys,"* Wiley, New York, (1972).

Barker J.F, Kreuger, D.D, and Change D.R, "Thermomechanical Processing of inconel 718 and its effect on properties", *Advanced High- Temperature Alloys: Processing and properties,* held in Cambridge, MA, June 16- 18, 1385 American society for metals, metals Park, OH, 125-137 (1986).

Inconel Alloy 718, *"Huntington Alloys",* Inc. 10M7-78 T- 39 (1978).

Ross E.W., and Sims C.T., *"Nickel Base Superalloys",* in: Superalloys II, C.T. Sims et al., (Eds.), pp. 97-131, (1987).

Special Metal data sheet for Inconel 625, publication number SMC-063, special metal corporathon, 200 (jan06).

Sindo Kou, *Welding Metallurgy, trans – Shamanian Ashrafi,* (2006) Isfahan University of Technology, Publication Center, First Edition.

Casti hand book of stainless steel and nickel alloy, fourth edition, 2001

Standard API 6A718 2006

Steven R.A., and Flewitt P.E.J., "Microstructural changes which occur during isochronal heat treatment of the nickel-base superalloy IN-738" J. Mat. Sci., vol. 13, No. 2, pp. 367-376, (1978).

Bhowal P.R., Wright E. F. and Raymond E.L., "Effects of cooling rate and γ′ morphology on creep and stress-rupture properties of a powder metallurgy superalloy", *Met. Trans. A,* 21A, 1709- 1717, (1990).

Shaw S.W.K. et al., "Response of IN-939 to process variations" in: Tien K. (Ed.), *Superalloys* 80, ASM, 275-284, (1980).

Pope D.P., and Ezz S.S., "Mechanical properties of Ni_3Al and nickel-base alloys with high volume fraction of gama" *International Metals Reviews,* 29(3), 136-167, (1984).

Delargy K.M., Shaw S.W.K., Smith G.D.W., "Effects of heat treatment on mechanical properties of high-chromium nickel-base superalloy IN 939", *Materials Sci. & Techn.,* 2(10), 1031-1037, (1986).

k.P. Cooper, P. Slebodnick, 1996," Seawater wear behavior of laser surface modified inconel 625 alloy ", *Material science and engineering A,* 206, 138-149.

A.S. Shahi, S. Pandy, (2008). Modeling of the effects of welding conditions on dilution of stainless steel cladding produced by gas metal arc welding procedures. *Journal of materials processing technology,* 196, 339-344.

H.M. Tawancy, I.M. Allam, N.M. Abas 1990, "Effect of ni3Nbprecipitation on the wear resistance of inconel alloy 625". *Material Science letters, 9,* 343-347.

Amadeh A.A. & Sadeghi Larijani M. (2009). Layering Martensite Stainless Steel with Cobalt and Nickel-based Alloys by GTAW and Investigating Its Wear Resistance. University of Tehran, College of Engineering.

W. Wu L. T. Wu 1996. "*The wear behavior between hard facing materials" A,* 27, 3639-3648.

Amadeh A. A. & Kashi H. (2004). Increasing the Lifespan of Hot Forging Dies through Hardening with Super Alloys by Welding. University of Tehran, College of Engineering.

Metals Handbook, *properties and selection: non-ferrous alloys and special purpose materials,* "ASM", 9thed, vol.2.

H.Y. Al-fadhli, J. Stokes, M.S.J. Hashmi, B.S. Yilbas, (2006),"The erosion-wear behavior of high velosityoxy-fuhl (HVOF) thermally sprayedinconell-625 coatings on different metallic surfaces", *Surface and Coating Technology* 200, 5782-5788

E.S. Puchi Cabrera, J.A. Berr'los- Ortiz, J. da-Silvab, J. Nunes, (2003), "fatigue behavior of a4140 steel coated with a Colmonoy 88 alloy applied by HVOF", *Surface and coatings technology* 172, 128-138.

D.Zhang, S.J.Harris, D.G. McCartney, (2003),"Microrostructure formation and wear behavior in HVOF-Sprayed Inconell 625 coatings", *Material Science and Engineer A,* 344, 45-46.

E.L. Hibner, D.B. O'donnell, (1994),"wear resistance of Inconel alloy725Weld Overlay", Inco Alloys International.

J.n.dupont, 1996, "Solidification of on alloy 625weld overlay", *Metallurgical and materials trancactions A,* 27A, 3612-3620.

Y. Takatani, T. Tomita K. Nagai, and Y. Harada, 1996, "wear behavior of Ni-Cr weld overlay alloys with dispersed," Carbide particles in sodium chloride solution. *Journal of thermal spray technology,* 5(3), 289-297.

Tadeusz Hejwowski, (2009), *"Erosive and abrasive wear resistance of overly coatings",* vacuum 83, 166-177.

Welding Handbook, AWS, vol, 4, Ninth edition.

F. Molleda, J. Mora F.J. Molerda, E. Carrillo, B.G. Mellor, 2006, *"A study of the solid- liquid inter face in the cobalt base alloy coating deposited by fusion welding (TIG).*

A.S.C.M.D. Oliveira, R.S.C. Paredes, 2006" Pulsed Current Plasma Transferred arc Hard facing" *journal of materials processing technology,*171, 167-174.

Monshi A. & Moradi R. (1999). *Metal Solidification.* Arkan Publication. Isfahan.

D.A. Porter, K.E. Easterling, 1992, *"Phase transformation in metals and alloys",* 318-312.

K.P. Cooper, P. Slebodnick, E.D. Thomas, 1996,"sea water wear behavior of laser surface modified Inconel 625 alloy ", *material science and engineering A*, 206, 138-149.

Jamali M., Honar A., Rauf B., & Heydarzadeh Sohi M. (2005). Surfacing Alloying on Steel AISI1045 with Chrome though TIG Process. *The 9th Congress of the Iranian Metallurgical Society*, 217-221.

J.N. Dupont, 1996, "solidification of on alloy 625 weld overlay", *Metallurgical and materials transactions A*, 27A, 3612-3620.

T. Sawai, Y. Ueshim, 1990. "Microsegeregation and Precipitation behavior z37during solidification in a nickel based super alloy", *ISIJ international*, 30(7), 520-523.

R.M. Nugent, 1986,"Alloy 625 Surfacing of tool and die steels", *welding Journal*, 33-39.

J.C. Shin, 2003, "Effect of molybdenum on the microstructure and wear resistance of the cobalt-base satellite hard facing alloys", *Surface and coatings technology*, 166, 117-126.

Satamert, H.K.DH. Bhadeshia,1989, *"Camparision of the microstructures and abrasive wear properties of satellite hard facing alloys deposited by arc welding and laser cladding"*. A 20, 1037-1054.